

Counterion Dynamics of κ - and ι -Carrageenan Aqueous Solutions Investigated by the Dielectric Properties

Makoto Takemasa* and Akio Chiba

Department of Applied Physics, School of Science and Engineering, Waseda University, 3-4-1 Okubo, Shinjuku-ku, Tokyo, 169-8555 Japan

Munehiro Date

Kobayasi Institute of Physical Research, 3-20-31 Kokubunji, Tokyo, 185-8533, Japan

Received February 7, 2002; Revised Manuscript Received April 18, 2002

ABSTRACT: The temperature dependence of the dielectric properties of κ - and ι -carrageenan aqueous solutions with various counterion species, K, Ca, and Na, were investigated over the frequency range 10^{-2} – 10^6 Hz and the temperature range 2.0–80.0 °C. In the case of κ -carrageenan solutions, just below the coil-to-helix transition temperature, T_{CH} , the dc conductivity sharply decreases within a few degrees of temperature. In contrast, the sharp decrease was not observed for ι -carrageenan solutions. The dielectric relaxation process with the relaxation time ~ 100 μ s, which can be assigned to the counterion fluctuation in the parallel direction to the helical axis, arises below T_{CH} . Just below T_{CH} , the relaxation strength increases sharply with decreasing temperature for both the carrageenan type with all the counterion species exhibiting the coil-to-helix transition, reaching $\sim 10^3$ at the temperatures far below T_{CH} . These findings indicate that the counterions are tightly bound to helical molecules due to an increase of the charge density along the helical axis during the coil–helix transition. The relaxation time reflecting the fluctuation distance increases sharply in the initial stage of gelation and gradually reaches a constant value. We think that the formation of the high charge density region, which is connected with the aggregated region of helices, is determined by which process, a growth of the length of the helices or the aggregation of the helices, precedes in the initial stage of gelation.

1. Introduction

Counterions play a very important role in the gelation of physically linked polyelectrolyte gels. An aggregation of helical molecules acts as a cross-link for a lot of physical gels such as carrageenan,¹ gellan,¹ agarose,² and pectin.³ It is important to clarify the binding nature of counterions for the better understanding of the aggregated region. Conductivity and dielectric measurements must be very strong tools to clarify the role of counterions in the formation of the cross-link in polyelectrolyte gels.

According to the Manning's counterion condensation theory,⁴ bound counterions are classified into two types, loosely and tightly bound counterions, in terms of the charge density along the polymer axis. The coil-to-helix conformational change of the polyelectrolyte induces an increase of the charge density of polyions and an increase of the bound counterions, which can be detected by the conductivity measurement. The increase of the charge density during the coil-to-helix transition causes an increase of the dielectric constant in connection with decreasing the contribution to the conductivity. The conductivity measurement offers information about the amount and mobility of the counterions moving through the charged polymer network, reflecting the electrostatic interaction between polyion and counterion. Since the loosely and tightly bound counterions are observed as a single type of bound counterions from the dc conductivity, dielectric measurements are quite useful to obtain the binding nature.

It is known that in the semidilute region two dielectric relaxation processes, the low-frequency (\sim kHz) and the

high-frequency (\sim MHz) processes, are observed for linear polyelectrolyte solutions such as DNA,⁵ poly(acrylic acid),⁶ and polyglutamate.⁷ The low frequency relaxation strongly depends on the degree of polymerization N , and the high-frequency one is nearly independent of N .^{8–10} According to Ito et al., the low- and high-frequency relaxations arise from the counterion fluctuations in the directions parallel and perpendicular to the polymer chain axis, respectively.^{11,12} The low-frequency relaxation is ascribed to the counterion fluctuation tightly bound to polyion and the high-frequency relaxation to the fluctuation of loosely bound counterions spreading over the average distance between polyions. When the dielectric relaxation arises from the counterion fluctuation, the relaxation time τ is characterized by $\tau \propto d^2/\mu$, where d is the fluctuation distance of the counterion and μ is the mobility of the counterion, which is proportional to the diffusion constant.¹³ The fluctuation distance estimated from the low-frequency process is expected to reflect the size of the high charge density region.

The carrageenans, the gelation mechanism of whose aqueous solutions we focused on in this study, are natural polysaccharide extracted from red algae. Their primary structures are based on an alternating disaccharide repeating unit of 1,3-linked β -D-galactose and 1,4-linked 3,6-anhydro- α -D-galactose. These aqueous solutions with specific cations form physically cross-linked thermoreversible polyelectrolyte gels. In carrageenan gels, the cross-linking has been considered as a side-by-side aggregation of helical molecules.^{14,15} The macroscopic properties of carrageenan gel are strongly affected by cation species.^{16–18} The cross-linking structure depends on the counterion species and amount of

* Corresponding author: e-mail takemasa@polymer.phys.waseda.ac.jp, Tel/FAX +81-3-5286-3194.

Table 1. Molar Ratio of Cation Content (%) in the Purified Samples to the Sulfur Content

	sodium	potassium	calcium	cesium
K-form	<0.89	85.17	0.10	13.84
Na-form	99.41	<0.01	0.43	0.15
Ca-form	2.23	0.77	86.68	10.32

added salt.¹⁹ The charge density of the carrageenan chain increases with decreasing temperature due to the temperature-induced coil-to-helix transition and the aggregation of helices. Then, the amount of the bound counterions increases, and the binding state of counterions changes in the sol–gel transition. The fluctuation distance of counterions reflects the size of the associated region of helical molecules. It is expected that a new physical insight into the cross-linking region of aggregated carrageenan helices is obtained from the investigation on the nature of free and bound counterions.

The high-frequency dielectric relaxation due to the bound counterions to carrageenan chains was observed by Ikeda et al.^{20,21} They showed that there is no specific binding of counterions in the random coil state. However, as far as we know, no systematic study on the low-frequency process of the carrageenan solutions seems to have been performed due to an experimental difficulty. The difficulty is caused by the electrode polarization and the high loss tangent due to the high dc conductivity.

We have reported that a rigid segment is essential for the gel network structure, and a number of aggregated helical molecules increases with decreasing temperature.²² The knowledge about the formation of the cross-linking region can be reinforced by the estimation of the longitudinal length of aggregation region by using the low-frequency dielectric relaxation measurements.

In this study, we focused on the low-frequency relaxation process and successfully measured the dielectric spectra during the sol-to-gel transition by an improvement of the apparatus. It was found that the dielectric properties in the gel state are quite different from those in the sol state, which indicates the difference of the nature of the bound counterions. The dielectric relaxation strength $\Delta\epsilon$ in the gel state reaches an order of 10^3 . The temperature dependence of the estimated fluctuation distance from the relaxation time increases sharply at the initial stage of gelation.

2. Experiments

2.1. Samples. κ - and ι -carrageenan from *Eucheuma cottonii* and Irish Moss, respectively, were purchased from Sigma Chemical Co. Ltd. The samples were purified by dialysis and deionized.²² We refined the potassium, sodium, and calcium-form κ - and K-form ι -carrageenan. The ratio of each cation content in the purified samples to sulfur content is listed in Table 1. The cation content was estimated by ion chromatography, and the sulfur content was estimated by inductively coupled plasma spectrometry.

2.2. Apparatus. We have extensively developed the apparatus of dielectric measurements. A schematic diagram of the apparatus is shown in Figure 1. This apparatus makes it possible to improve an accuracy of the measurements for polyelectrolyte solutions at low frequencies, reducing a difficulty resulting from the high loss tangent due to high dc conductivity.

The imaginary part of the complex permittivity ϵ'' for the solutions exhibiting high dc conductivity obeys σ/ω over a wide

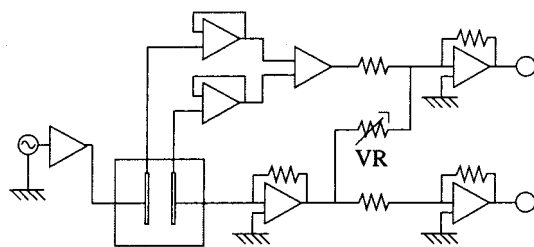


Figure 1. A schematic diagram of the apparatus for the dielectric measurements. The dc conductivity component is canceled by using the variable resistor (VR) before the amplification and digitizing of the signal in order to estimate the real part of complex permittivity accurately.

frequency range. At low frequencies, an electrode polarization effect resulting from an accumulation of charges near the electrode causes an increase of the ϵ' and ϵ'' with decreasing frequency.²³ Therefore, at the lower frequency, accurate measurements become more difficult. In this study, $\tan \delta$ reaches more than 10^3 near the frequency 10^4 Hz. We tried to cancel the dc conductivity component by using the variable resistor (VR) shown in Figure 1 before the amplification and digitizing of the signal in order to measure the real part of complex permittivity accurately. The amplitude of the voltage applied to the sample, the current, and the phase angle between the voltage and the current were recorded. The complex permittivity was calculated from the amplitudes and the phase angle using the parallel-plate approximation.

The dielectric measurement was performed in the frequency range 10 mHz–100 kHz by the use of the apparatus in Figure 1 and in the 1 kHz–1 MHz range with an HP4284A impedance analyzer. We have confirmed that the experimental data obtained by the two apparatus agree with each other in the overlapping frequency range 1 kHz–100 kHz. We used the parallel-plate electrodes made of platinum black. A temperature control was made by LAUDA RCS with an accuracy of ± 0.1 °C. The sample was poured into the cell in the sol state and kept at 90 °C for 30 min to dissolve completely.

3. Results

Figure 2 shows the temperature dependence of dielectric dispersion ϵ' spectrum for (a) 1.0 wt % Ca-form and (b) 1.0 wt % Na-form κ -carrageenan solutions in the frequency range 10^{-2} – 10^6 Hz in the temperature range 5–60 °C. In the case of Ca-form κ -carrageenan solution, the frequency dependence of ϵ' shows the characteristic behavior in the temperature range lower than 9.5 °C, corresponding to the coil–helix transition temperature. In the case of the sample with nongelling promoting cation of Na, which does not show the coil–helix transition at this ionic concentration,¹⁹ such behavior was not observed.

The ϵ' and ϵ'' spectrum of 1.0 wt % Na-form κ -carrageenan solution at 60 °C is shown in Figure 3. The ϵ'' obeys $\epsilon'' \sim 1/\omega$ in the wide frequency range 10 Hz–1 MHz, which means that the dc conductivity is a dominant effect in this frequency region. The electrode polarization effect ϵ_{ep}^* is represented by the empirical function²³

$$\epsilon_{el}^* = \frac{\epsilon_{ep}}{(j\omega)^\gamma} \quad (1)$$

where ω is the angular frequency and ϵ_{ep} and n the electrode polarization parameter. The ϵ' exponentially increases with decreasing frequency below $\sim 10^3$ Hz due to electrode polarization. We used the equation including the effects of the dc conductivity and the electrode

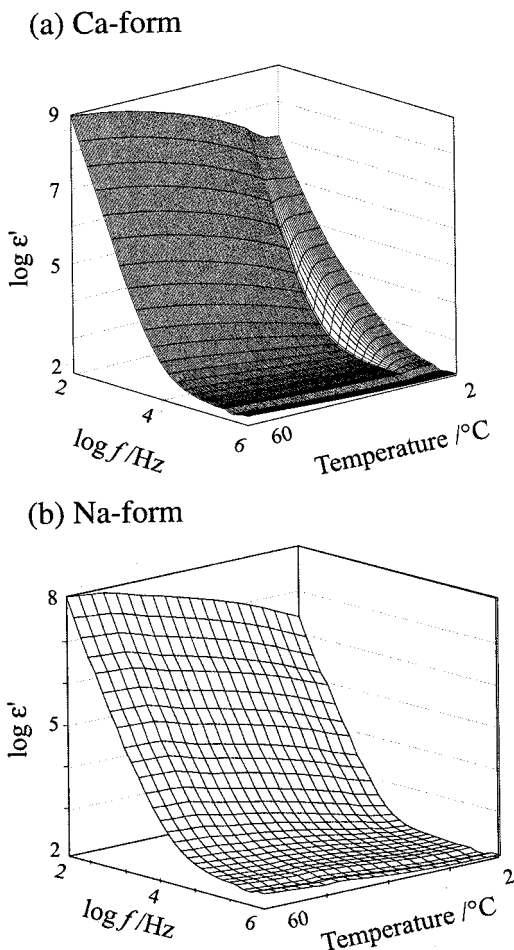


Figure 2. Temperature dependence of the dielectric dispersion ϵ' spectrum of (a) 1.0 wt % Ca-form and (b) 1.0 wt % Na-form κ -carrageenan.

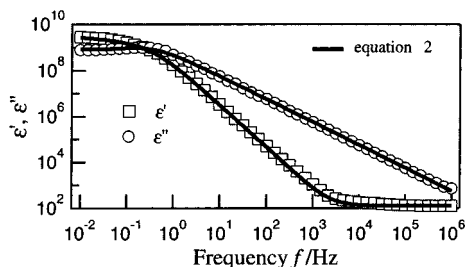


Figure 3. Temperature dependence of the dielectric dispersion ϵ' and loss ϵ'' of 1.0 wt % Na-form κ -carrageenan at 60 °C. The solid line was calculated from eq 2 by the least-squares fitting procedure.

polarization to reproduce the experimental data

$$\epsilon^* = \frac{1}{\frac{1}{\epsilon_\infty + \frac{\sigma}{i\omega}} + \frac{(i\omega)^\gamma}{\epsilon_{ep}}} \quad (2)$$

where ϵ_∞ is the instantaneous permittivity and σ the dc conductivity. In the sol state, we can reproduce the data using eq 2 as a result of the nonlinear least-squares fitting procedure, as shown in Figure 3, which indicates that the dc conductivity and the electrode polarization are dominant in this temperature.

Figure 4 shows the frequency dependence of ϵ' and ϵ'' of 1.0% Ca-form κ -carrageenan at (a) 60 °C and (b) 5

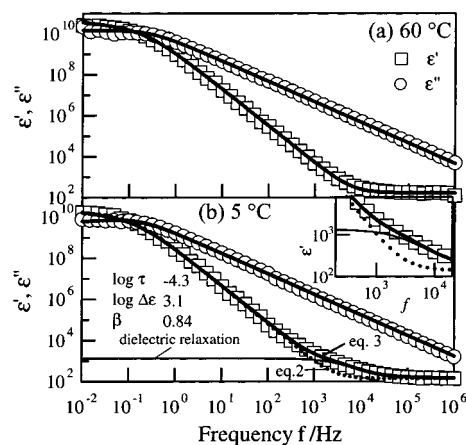


Figure 4. Temperature dependence of the dielectric dispersion ϵ' and loss ϵ'' of 1.0 wt % Ca-form κ -carrageenan at (a) 60 °C and (b) 5 °C. The thick solid, the dotted, and the thin solid lines represent the best-fitted curve with eq 3, the fitted curve with eq 2, and the relaxation term in eq 3, respectively. An inset shows the magnified view around 10^3 Hz.

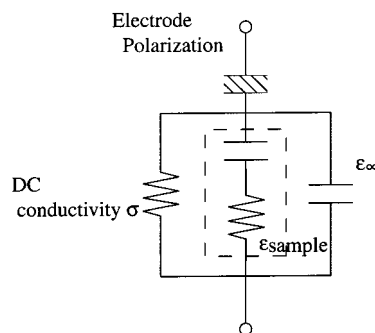


Figure 5. Equivalent circuit of eq 3 for reproducing the observed spectra.

°C in the cooling process, which correspond to the coil and helical state, respectively.¹⁹ We can reproduce the data at 60 °C with eq 2. However, at 5 °C we cannot reproduce the data with eq 2. We found that a systematic deviation between the observed ϵ' and the fitting curve calculated from eq 2 in the frequency range $10^{2.5}$ – $10^{4.5}$ Hz. Only an addition of the relaxation term gave an excellent fit.

$$\epsilon^* = \frac{1}{\frac{1}{\epsilon_\infty + \frac{\Delta\epsilon}{1 + (i\omega\tau)^\beta} + \frac{\sigma}{i\omega}} + \frac{1}{\frac{\epsilon_{ep}}{(i\omega)^\gamma}}} \quad (3)$$

$\Delta\epsilon \equiv \epsilon_0 - \epsilon_\infty$

where ϵ_0 is the static permittivity, τ the relaxation time, and β the distribution parameter of the relaxation time in the Cole–Cole dielectric relaxation function.²⁴ The equivalent circuit of eq 3 is shown in Figure 5.

Figure 6 shows the temperature dependence of the dc conductivity σ for K-, Ca-, and Na-form κ -carrageenan solutions and for K-form ι -carrageenan solution. σ decreases with decreasing temperature for all the samples. For the κ -carrageenan solutions having gelation promoting counterions of K and Ca, a sharp decrease of σ was observed in a few degrees of temperature just below the coil–helix transition temperature T_{CH} . On the contrary, the sharp decrease at T_{CH} was not observed in the case of ι -carrageenan. The temper-

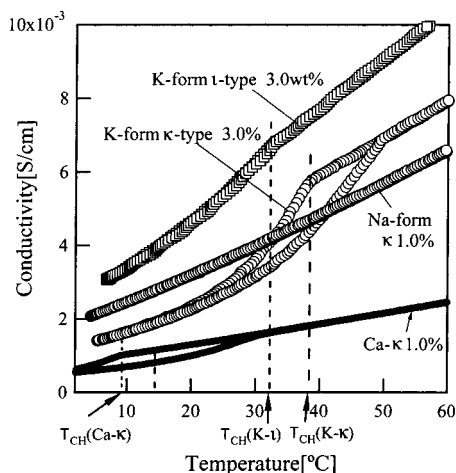


Figure 6. Temperature dependence of the dc conductivity σ for K-, Ca-, and Na-form κ - and K-form ι -carrageenan solutions in the temperature range 2.0–80.0 °C. The dotted line of the vertical direction represents the coil-to-helix transition temperature T_{CH} for each sample.

Table 2. Coil-to-Helix Transition Temperatures of the Investigated Samples in the Cooling Process Estimated from dc Conductivity^a

	K-form κ	Ca-form κ	K-form ι
$T_{C-H}/^{\circ}\text{C}$	37.8	9.5	32.4

^a Na-form κ -carrageenan aqueous solution does not exhibit the coil–helix transition.

ature region where a thermal hysteresis was observed in the dc conductivity was quite different for ι - and κ -carrageenan and does not depend on the counterion species. This result is consistent with the suggestion that the thermal hysteresis is affected mainly by the carrageenan type, or in other words, a charge density of polyion, and is caused by the aggregation of the helices.²⁵ The coil-to-helix transition temperatures of the investigated samples in the cooling process estimated from dc conductivity are listed in Table 2.

A typical temperature dependence of the dielectric relaxation parameters, τ , $\Delta\epsilon$, β , and ϵ_{∞} , and the electrode polarization parameters, γ and ϵ_{ep}^* , of Ca-form κ -carrageenan estimated by the least-squares fitting procedure are shown with the residual of the fit in Figure 7. In the helix state, the residual resulting from the fitting procedure with eq 2 is much larger than that with eq 3. We used eq 3 for the helix state and used eq 2 for the coil state. γ and ϵ_{∞} are almost temperature-independent. τ and $\Delta\epsilon$ exhibit a thermal hysteresis in the helix state.

Figure 8 shows the temperature dependence of τ and $\Delta\epsilon$ for Ca- and K-form κ -carrageenan and for the K-form ι -carrageenan aqueous solutions. In the cooling process, both τ and $\Delta\epsilon$ sharply increase just below T_{CH} , corresponding to the initial stage of gelation, and gradually reach a constant value at low temperatures for all the gelled samples. A large thermal hysteresis was observed for K-form and Ca-form κ -carrageenan. In contrast, almost no thermal hysteresis was observed for K-form ι -carrageenan.

4. Discussion

The dc conductivity measurement has been used for detecting the conformational transition of carrageenan aqueous solutions. According to Rochas and Landry,²⁶

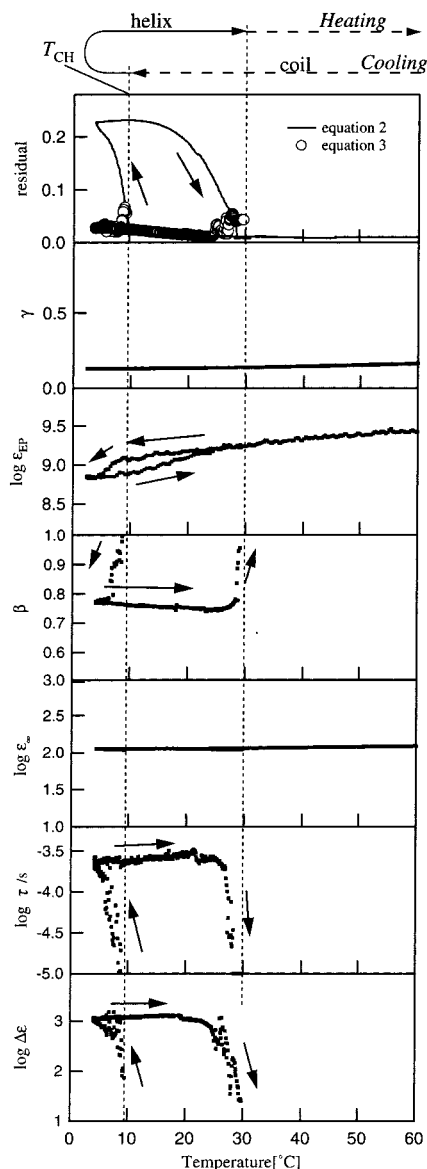


Figure 7. A typical temperature dependence of the dielectric relaxation parameters; the relaxation strength $\Delta\epsilon$, the relaxation time τ , and the distribution parameter of the relaxation time in the Cole–Cole relaxation function β , the residual resulting from the fitting procedure, and the electrode polarization parameters ϵ_{ep} and γ of 1.0 wt % Ca-form κ -carrageenan solution. All the measurements were carried out under the thermal condition that the sample was cooled from 80 to 2 °C and then heated from 2 to 80 °C. The path of the thermal treatment is summarized over the top of the graph. The dotted and the solid line correspond to the coil and helix state, respectively.

the ratio of the equivalent conductivity of the carrageenan aqueous solution to the simple electrolyte aqueous solution such as KCl solution of the same ionic concentration gives information about the conformation of the polymer chains just corresponding to the optical rotation results.

The conductivity σ is described as

$$\sigma = \sum |z_i| F^2 c_i \mu_i \quad (4)$$

where z_i is the valence of the i th ion, F the Faraday constant, c_i the local concentration, and μ_i the mobility. The summation covers all the ionic species. Using the

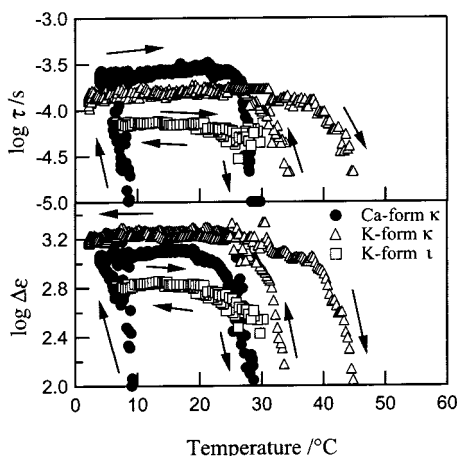


Figure 8. Temperature dependence of $\Delta\epsilon$ and τ of Ca- and K-form κ -carrageenan and K-form ι -carrageenan aqueous solutions.

relation between the mobility and diffusion coefficient,

$$\mu_i = \frac{D_i}{kT} \quad (5)$$

where D_i is the diffusion coefficient of i th ion, k the Boltzmann constant, and T the absolute temperature, eq 4 is rewritten as

$$\sigma = \frac{F^2}{kT} \sum |z_i| c_i D_i \quad (6)$$

σ decreases with decreasing temperature for all the samples, as can be seen in Figure 6. The main origin of this phenomenon is the decrease of D_i .²⁷ In the case of 1.0 wt % Na-form κ -carrageenan aqueous solution, which is in the coil state in the entire temperature range, σ decreases with decreasing temperature, and no significant change of σ was observed in the entire temperature range, as shown in Figure 6. This means that only the diffusion coefficient decreases with decreasing temperature, and the binding nature of the counterions does not change.²⁷

In contrast, in the case of the sample exhibiting the coil-to-helix transition, K- and Ca-form κ -carrageenan, a sharp decrease of σ was observed just below T_{CH} . According to Clszkowska et al., the conductivity of the simple electrolyte aqueous solution (NaCl) is much higher than that of carrageenan solution with the same cations, which indicates that the diffusion coefficient of polyions is much smaller (~ 2 orders) than that of Cl^- . A fraction of cations is condensed onto the polyion, and the diffusion coefficient of the condensed cations is very low.²⁷ We think the abrupt decrease of the dc conductivity results from the binding of the counterions. The dielectric relaxation was observed for the samples exhibiting the coil-to-helix transition at the temperatures lower than T_{CH} , as shown in Figure 6. This is strong evidence that the dielectric relaxation arises due to a change of the binding nature of the counterions accompanied by the coil-to-helix transition.

According to the Manning's counterion condensation theory,⁴ the bound counterion to polyion is classified into two types, the loosely and tightly bound counterions, in terms of the dimensionless charge density parameter ξ defined as

$$\xi = \frac{e^2}{\epsilon b k T}$$

where b is the charge separation distance, e the elementary of electric charge, ϵ the dielectric constant of solvent, k the Boltzmann constant, and T the temperature. The tightly bound counterions arise when ξ is higher than $1/z$, where z is the counterion valence.⁴ For example, when the counterion is monovalent, if $\xi < 1$, all the bound counterions are classified into the loosely bound counterion. If $\xi > 1$, the counterion tightly bound to polyion arises.

During the coil-helix transition, the charge separation distance b becomes shorter, which induces the increase of ξ . The values of b for the coil and double-helical state in the carrageenan aqueous solutions, which were estimated by the chemical structure of the monomers and the helical structure using X-ray data,^{28,29} are listed in Table 3. If we assume that the structure of carrageenan molecules in aqueous solution is a double helix, we can obtain $\xi_{\text{coil}} \sim 0.68$ and $\xi_{\text{helix}} \sim 1.65$ for coil and the helical state, respectively, in κ -carrageenan aqueous solutions. The temperature dependence of the dc conductivity showed that the coil and helix coexist in the solution at the temperatures below T_{CH} , and the helical content increases with decreasing temperature. $\xi_{\text{helix}} = 1.65$ anticipates that the tightly bound counterions to the helical segment appear below T_{CH} and increase with decreasing temperature.

Since the dielectric relaxation arises just below T_{CH} , and the relaxation strength increases with decreasing temperature, this relaxation should be connected with the change of binding nature of the counterions and the appearance of tightly bound counterions. According to Ito et al., the dielectric relaxation process was also observed at low frequencies ($\sim \text{kHz}$) for the linearly charged polyelectrolyte aqueous solutions and is ascribed to the fluctuation of counterions tightly bound to polyions along the polyion axis.^{11,12} The relaxation time τ for the process is proportional to d^2/μ , where μ is the mobility of the counterion and d is the fluctuation distance of the counterion.¹³

Let us consider the relaxation mechanism of the low-frequency process in relation to the gelation of carrageenan solutions. The cross-linking mechanism of carrageenan gels is considered as a side-by-side aggregation of helical molecules.^{14,15} Since the macroscopic properties, such as optical, mechanical, and electrical properties, of carrageenan gel are strongly affected by cation species,^{16–19} it is suggested that the cross-linking structure, such as the longitudinal length of the aggregated region and the number of helices bundled in a cross-linking region, depends on counterion species and the amount of added salt. Since the relaxation time τ of the low-frequency process corresponds to the fluctuation distance d of tightly bound counterions, in the case of carrageenan gels τ reflects the size of the high charge density region. We can discuss the change of the longitudinal length of the aggregated region by the temperature dependence of τ . We have already reported that, in terms of the correlation between the shear modulus and the strain optical coefficient, the stress inducing the polymer chain orientation, especially of the helical molecules, increases with decreasing temperature during the formation process of the gel network.²² The length of the rigid segment, the helical molecule, is important for enlarging the stress for the orientation.

Table 3. Charge Separation Distance from the Literature of the Random Coil and Double-Helical Structure^a

		<i>b</i> /Å
kappa	random coil	10.0
	double helix	4.3
iota	random coil	5.0
	double helix	2.15

^a The *b* for the random coil state is estimated from fully extended molecular models, and the *b* for the double helix is estimated from the X-ray diffraction data.^{28,29}

Figure 8 shows that the relaxation time sharply becomes longer in the initial stage of gelation and gradually reaches a constant value at low temperatures for all the gelled samples. In terms of this behavior, the longitudinal length of the helices and their aggregated region sharply increase in the initial stage of gelation and gradually reaches a constant value at low temperatures. This result supports the conclusion of the previous study that the enlargement of the stress inducing the polymer orientation is mainly caused by the increase of the number of helical molecules bundled in a cross-linking region.

Judging from the fact that $\Delta\epsilon$ increases sharply just below T_{CH} and reaches gradually a constant value at low temperatures, the cross-linking and the gel network structure are dominated by which process, a growth of the length of the helices or the aggregation of the helices, precedes in the initial stage of gelation. At the initial stage of gelation, in other words, just below T_{CH} , some short helices appear in a chain. When the aggregation rapidly occurs just below T_{CH} and the gel network is formed before the growth of the long helices, the longitudinal length of the aggregated region is hard to increase due to the constraint by the other chains in the network. The long helices can be formed when the growth of the long helix occurs before the helices are taken part in the gel network.

In the case of κ -carrageenan, the tightly bound counterion appears at $T < T_{CH}$, since the helical segment with $\xi > 1$ appears at $T < T_{CH}$. In contrast, for ι -carrageenan, $\xi > 1$ even in the coil state. The tightly bound counterion should exist in the entire temperature range, which was experimentally supported by Ueda et al.³⁰ However, in this study, the dielectric relaxation was not apparently observed in the coil state, as shown in Figure 8. We think that the relatively short fluctuation length of the tightly bound counterions causes this situation.

Acknowledgment. The authors are grateful to Dr. Takaaki Sato for helpful discussion and to Professor

Takeo Furukawa of Science University of Tokyo for a valuable comment on the equivalent circuit for the relaxation model. This work is partly supported by the grant-in-aid for scientific research from Japan Society for the Promotion of Science.

References and Notes

- (1) Piculell, L. *Curr. Opin. Colloid Interface Sci.* **1998**, *3*, 643–650.
- (2) Djaburov, M.; Clark, A. H.; Rowlands, D. W.; Ross-Murphy S. B. *Macromolecules* **1989**, *22*, 180–188.
- (3) Pilnik, W.; Rombouts, F. M. *Carbohydr. Res.* **1985**, *142*, 93–105.
- (4) Manning, G. S. *J. Chem. Phys.* **1969**, *51*, 924–933.
- (5) Uemura, S.; Hayakawa, R.; Wada, Y. *Biophys. Chem.* **1980**, *11*, 317–320.
- (6) van der Touw, F.; Mandel, M. *Biophys. Chem.* **1974**, *2*, 231–241.
- (7) Muller, G.; van der Touw, F.; Zwolle, S.; Mandel, M. *Biophys. Chem.* **1980**, *11*, 317–320.
- (8) Minakata, A.; Imai, N. *Biopolymers* **1972**, *11*, 329–346.
- (9) Muller, G.; Van der Touw, F.; Zwolle, S.; Mandel, M. *Biophys. Chem.* **1974**, *2*, 242–254.
- (10) Mandel, M.; Odjik, T. *Annu. Rev. Phys. Chem.* **1984**, *35*, 75–108.
- (11) Ito, K.; Yagi, A.; Ookubo, N.; Hayakawa, R. *Macromolecules* **1990**, *23*, 857–862.
- (12) Ookubo, N.; Hirai, Y.; Ito, K.; Hayakawa, R. *Macromolecules* **1989**, *22*, 1359–1366.
- (13) Oosawa, F. *Polyelectrolytes*; Marcel Dekker: New York, 1971.
- (14) Morris, E. R.; Rees, D. A.; Robinson, G. *J. Mol. Biol.* **1980**, *138*, 349–362.
- (15) Hermansson, A. M. *Carbohydr. Polym.* **1989**, *10*, 163–181.
- (16) McKinnon, A.; Rees, D. A.; Williamson, F. B. *J. Chem. Soc., Chem. Commun.* **1969**, 701–702.
- (17) Rochas, C.; Rinaudo, M.; Vincendon, M. *Biopolymers* **1980**, *19*, 2165–2175.
- (18) Ablett, S.; Clark, A. H.; Rees, D. A. *Macromolecules* **1982**, *15*, 597–602.
- (19) Rochas, C.; Rinaudo, M. *Biopolymers* **1980**, *19*, 1675–1687.
- (20) Ikeda, S.; Kumagai, H.; Nakamura, K. *Food Hydrocolloids* **1997**, *11*, 303–310.
- (21) Ikeda, S.; Kumagai, H. *J. Agric. Food Chem.* **1998**, *46*, 3687–3693.
- (22) Takemasa, M.; Chiba, A.; Date, M. *Macromolecules* **2001**, *34*, 7424–7434.
- (23) Johnson, J. F.; Cole, R. H. *J. Am. Chem. Soc.* **1951**, *73*, 4536–4540.
- (24) Cole, K. S.; Cole, R. H. *J. Chem. Phys.* **1941**, *9*, 341–351.
- (25) Piculell, L. In *Food Polysaccharides and Their Applications*; Stephen, A. M., Ed.; Marcel Dekker: New York, 1995, pp 205–244.
- (26) Rochas, C.; Landry, S. *Carbohydr. Polym.* **1987**, *7*, 435–447.
- (27) Clszkowska, M.; Kotlyar, I. *Anal. Chem.* **1999**, *71*, 5013–5017.
- (28) Anderson, N. S.; Campbell, J. W.; Harding, M. M.; Rees, D. A.; Samuel, J. W. B. *J. Mol. Biol.* **1969**, *45*, 85–99.
- (29) Arnott, S.; Scott, W. E.; Rees, D. A.; McNab, C. G. A. *J. Mol. Biol.* **1974**, *90*, 253–267.
- (30) Ueda, K.; Sato, S.; Ochiai, H.; Imamura, A. *J. Phys. Chem. B* **1997**, *101*, 3653–3664.

MA020206F